



Article

Multitemporal Remote Sensing Based on an FVC Reference Period Using Sentinel-2 for Monitoring *Eichhornia crassipes* on a Mediterranean River

Youssef Ghousein ^{1,2,3,4}, Hervé Nicolas ^{1,*} , Jacques Haury ², Ali Fadel ³, Pascal Pichelin ¹, Hussein Abou Hamdan ⁴ and Ghaleb Faour ³ 

¹ Agrocampus Ouest, UMR Sol Agronomie Spatialisation (UMR SAS), P.O. Box 35042 Rennes, France

² Agrocampus Ouest, UMR Ecology and Ecosystem Health (UMR ESE), P.O. Box 35042 Rennes, France

³ National Center for Remote Sensing, National Council for Scientific Research, P.O. Box 11-8281, Riad El Solh, 1107 2260 Beirut, Lebanon

⁴ Lebanese University, Faculty of Sciences (I), Rafic Hariri campus, P.O. Box, 14-6573 Beirut, Lebanon

* Correspondence: herve.nicolas@agrocampus-ouest.fr; Tel.: +33-2-23-48-55-52

Received: 11 July 2019; Accepted: 6 August 2019; Published: 9 August 2019



Abstract: Invasive aquatic plants are a serious global ecological and socio-economic problem because they can cause local extinction of native species and alter navigation and fishing. *Eichhornia crassipes* (water hyacinth) is a dangerous invasive floating plant that is widely distributed throughout the world. In Lebanon, it has spread since 2006 in the Al Kabir River. Remote sensing techniques have been widely developed to detect and monitor dynamics and extents of invasive plants such as water hyacinth over large areas. However, they become challenging to use in narrow areas such as the Al Kabir River and we developed a new image-analysis method to extract water hyacinth areas on the river. The method is based on a time series of a biophysical variable obtained from Sentinel-2 images. After defining a reference period between two growing cycles, we used the fractional vegetation cover (FVC) to estimate the water hyacinth surface area in the river. This method makes it possible to monitor water hyacinth development and estimate the total area it colonizes in the river corridor. This method can help ecologists and other stakeholders to map invasive plants in rivers and improve their control.

Keywords: *Eichhornia crassipes*; remote sensing; soil-adjusted vegetation index; FVC reference period; Sentinel-2; time series; Lebanon

1. Introduction

Invasive aquatic plants colonize aquatic ecosystems and alter their dynamics and biodiversity. That form of biological alteration is related to global climate change, which accelerates the extinction of native species [1,2]. *Eichhornia crassipes* (Mart.) Solms (water hyacinth) is one of the most dangerous invasive species in the world, as documented by several European and international organizations, such as the European and Mediterranean Plant Protection Organization and the International Union for Conservation of Nature [3–6].

Water hyacinth is a vigorous perennial plant that has been introduced mainly for ornamental purpose. Once it finds the right conditions to develop, it quickly colonizes watercourses and other water bodies, forming a dense green mat. As a result, it modifies habitats of native species, interrupts the passage of sunlight and depletes oxygen in aquatic environments, alters food chains and nutrient cycles, and causes a loss of water by evapotranspiration [7–9]. It has a wide geographic distribution. From its native habitat in Brazil, water hyacinth has spread to countries on all continents but Antarctica (Table 1).

Table 1. Geographic distribution of *Eichhornia crassipes* (water hyacinth).

Continent	Country	Location	References
North and South America	Bolivia	Dam of the San Jacinto	[10]
	Colombia	Lagoons outside the Amazon	[10]
	Mexico	Chapala and Guadalupe lakes	[10]
	USA	Rio Grande River	[11]
	USA	Sacramento–San Joaquin River	[12,13]
Africa	Angola	Kwanza River	[10]
	Egypt	Nile River	[14]
	Kenya	Lake Victoria	[15,16]
	Mali	Niger River	[10]
	Niger	Niger River	[10]
	Nigeria	Niger River: Nun River	[10,17]
	Zimbabwe	Manyame River: Manyame Lake and Inland Lake	[3,18]
Asia	China	Yangtze River	[10,19]
	India	Brahmaputra Assam River	[20,21]
	Turkey	Asi River	[22]
	Syria	Al Kabir River	[23,24]
	Lebanon	Al Kabir River	[23,24]
Europe	Spain	Guadiana River	[7,25]
	Portugal	Sado, Sorraia River, part of Tagus basin	[25–27]
	Germany	Erft River	[25,26]
	Italy	Sardinia and Lazio	[26–29]
	France	Moselle valley	[30]
Australia	Australia	Burdeki River	[31]

In the Eastern Mediterranean region, it has colonized many countries, such as Turkey, Lebanon, and Syria. Since 2006, it has colonized the Al Kabir River, which forms the natural border between Lebanon and Syria [24]. The river is an important water resource for the Akkar region but it faces several problems, such as pollution from untreated wastewater and solid waste. Water hyacinth is, therefore, a major environmental threat to both water quality and quantity [24,32,33]. Over the past 30 years Earth observation systems have provided data at a variety of spatial and temporal resolutions to map the distribution of vegetation cover, detect macrophytes, and monitor aquatic invasive plants [3,34]. According to the literature, many authors have confirmed the effectiveness of remote sensing tools. Multispectral and hyperspectral satellites, such as HyMap airborne, Spot 5, and Landsat 7 and 8, are widely used to detect aquatic vegetation [35].

Among hyperspectral approaches to invasive plants, Hestir et al. [13] used HyMap airborne hyperspectral images, high spatial resolution (3 m) to map invasive weeds, including *Lepidium latifolium* L., water hyacinth, and submerged aquatic vegetation in the Sacramento–San Joaquin River Delta of California, USA. They used regression models, spectral mixture analysis, and spectral angle mapping to map these plants, with different degrees of accuracy. Santos [36] monitored spatial and temporal dynamics of *Egeria densa* Planchon and water hyacinth in the same river delta. They used airborne hyperspectral data from 2003–2007 to assess effects of herbicide treatments used to manage these plants.

Among multispectral approaches of invasive plants, Jakubauskas et al. [37] used the high spatial resolution of the IKONOS (4 m) and ASTER satellites (15 m) to assess the ability to use their data to map two aquatic invasive plants (water hyacinth and *Hydrilla verticillata* (L.F.) Royle) in the lower Rio Grande River, in Texas, USA. They determined the correlation between percent plant cover and spectral reflectance data measured with a spectroradiometer. Their results showed that the remote sensing technology had significant potential to detect, monitor, and manage areas colonized by these plants.

Everitt and Yang [38] used QuickBird satellite images (2.8 m resolution) to distinguish between water hyacinth and *Pistia stratiotes* L. (water lettuce) in a large reservoir in southern Texas. They obtained similar accuracy in mapping water hyacinth using supervised or unsupervised classification (73–100% and 74–100%, respectively).

Mund et al. [16] tested a multi-sensor approach using MERIS (300 m resolution), MODIS (250 m), and Landsat 7-ETM (30 m) images to quantify and monitor the floating biomass on two tropical water bodies. Inle Lake, the second largest lake in Myanmar, and Lake Victoria in Kenya are both colonized by water hyacinth. The normalized difference vegetation index (NDVI) was used to quantify biomass.

Oyama et al. [39] used the medium resolution (30 m) of multispectral Landsat 7 TM and ETM+ shortwave infrared bands to distinguish cyanobacterial blooms from aquatic macrophytes in three Japanese lakes. Detection in these bands was most accurate using a combination of the floating algal index and the normalized difference water index.

Similarly, Fadel et al. [40] estimated chlorophyll-*a* concentrations in the Karaoun Reservoir in Lebanon using Landsat 8 Operational Land Imager (OLI) data (30 m resolution) to monitor algal blooms. The most accurate detection ($R^2 = 0.72$) was obtained by combining bands (B2:B4 ratio×B5)

Dube et al. [41] compared the ability of Landsat 8 and Landsat 7 ETM+ to detect and distinguish water hyacinth from other land cover types in Chivero Lake in Zimbabwe. Detection of water hyacinth cover had optimal accuracies of 92% compared to other land cover types based on Landsat 8 OLI data.

Pinardi et al. [42] used multispectral data acquired by the Sentinel-2A satellite to assess intra-annual spatial and temporal dynamics of allochthonous and invasive macrophyte species in a shallow lake system in Italy. The macrophyte mapping method is based on the Leaf Area Index (LAI). Their method mapped the macrophytes well using the leaf area index. Thamaga et al. [3] reviewed studies on the detection of water hyacinth using hyperspectral and multispectral data and vegetation indices. Generally, the studies used satellite images (e.g., Landsat) with high spatial resolutions to map and monitor large colonized areas. Conversely, the 10 m spatial resolution of Sentinel-2 is considered useful and more appropriate for monitoring water hyacinth on narrow colonized water bodies [3].

In our study, we used Sentinel-2 images to assess their potential to detect water hyacinth in the geographically narrow corridor of the Al Kabir River. Thus, in this applied study, our main objective was to map and monitor the area colonized by water hyacinth for four years (August 2015–December 2018). Doing so required distinguishing water hyacinth from riparian vegetation by developing an innovative method of remote sensing to map water hyacinth at an appropriate scale.

We focused on the vegetative cycles and seasonality of riparian vegetation and water hyacinth. We hypothesized that both can be distinguished spatially and temporally to identify a reference period of separation. Once this period was defined, we extracted information from 10×10 m pixels of Sentinel-2 images along the river and we used fractional vegetation cover (FVC) to determine temporal dynamics of water hyacinth.

2. Materials and Methods

2.1. Study Area

The Al Kabir River is a coastal Mediterranean river located on the northern border of Lebanon (Figure 1). It is 46 km long and fed by several tributaries, such as the Al Arousse. The Al Kabir watershed has a Mediterranean winter precipitation regime and dry-hot summer climate. The Al Kabir

River is under anthropogenic stress due to the uncontrolled discharge of untreated wastewater and solid waste deposits, resulting in environmental degradation and a serious threat to public health [24,32,33].

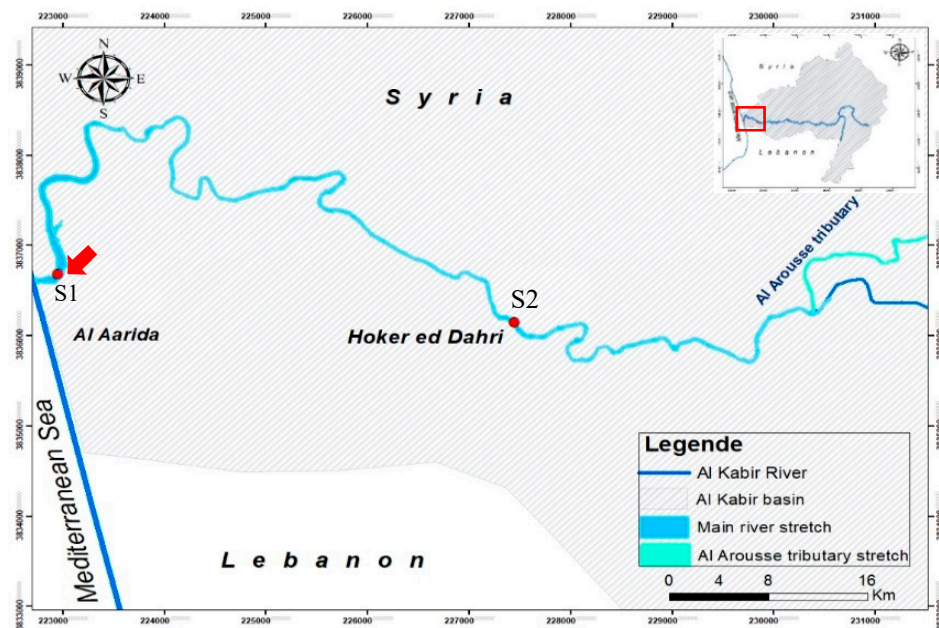


Figure 1. Al Kabir watershed and the study area. The red arrow indicates the two consecutive sectors used to distinguish water hyacinth and riparian vegetation cycles.

Water hyacinth was first recorded on the river in 2006 after being introduced from the Al Arousse tributary. It now extends from this tributary to the estuary, blocking irrigation canals of the tributary and the river.

Two accessible sites, Al Aarida (S1), located 400 m from the estuary, and Hoker ed Dahri (S2), located 9 km from the estuary, were observed in situ. These 100 m long sites were visited monthly in 2017 (April–November) and 2018 (May–June) to inventory the plant species present and observe changes in vegetation. During surveys, we observed seasonal variability and differences in vegetation development cycles and listed the plants growing in the riverbed and on the Lebanese bank.

2.2. Distinguishing Riparian and Water Hyacinth Cycles: Building the Reference Image

We first assumed that the growing cycles of water hyacinth and riparian vegetation are distinct during the year. In-situ observations suggest that riparian vegetation develops from February to mid-April and that water hyacinth develops later and is dominant over other amphibious plant species. This hypothesis will be evaluated with the results obtained by remote sensing. This distinction between vegetative cycles allows us to identify an intermediate period, from mid-April to mid-May, when riparian vegetation seems stabilized and water hyacinth has not yet developed. This period will be considered as a “reference period” in the evolution of vegetation in the river corridor. It is then necessary to know the vegetative development at this reference time to quantify the subsequent increase in vegetative surface area that will be mainly due to water hyacinth. This spatial information is required annually, but the availability of Sentinel-2 images is not systematically ensured according to cloudiness. We therefore analyzed the possibility of creating a computer-generated image using the images available during this reference period from 2015 to 2018. The stability of this reference image takes into account the interannual variability of the state of vegetative development in the river corridor.

2.2.1. Estimating Vegetation Cover

- Vegetation Indices

To exploit satellite-image data, vegetation indices are used to estimate vegetation cover. In this context, several authors [16,43,44] have shown the value of vegetation indices for detecting, identifying, or monitoring plant dynamics. These indices are linked to biophysical variables of plants such as biomass, growth stage, leaf index area, and water stress.

NDVI [44] is the one of the indices used most often; however, it is sensitive to atmospheric characteristics and optical properties of the soil [45–48]. Consequently, the soil adjusted vegetation index (SAVI) was developed [48] to minimize the influence of ground and water reflectance. Almutairi et al. [49] compared SAVI and NDVI in the Sulaibiya region of Kuwait using WorldView satellite data and found that SAVI determined vegetation cover in this arid region more accurately.

Fractional vegetation cover (FVC) is a biophysical parameter used to describe and estimate vegetation cover [50,51]. It can be calculated using either vegetation indices (e.g., NDVI, [50]) or algorithms [52,53].

- Choice of Fractional Vegetation Cover

Recent studies have shown the usefulness of FVC, among other available biophysical variables or vegetation indices, in estimating vegetation area [52,53]. In the preliminary tests of our study, NDVI showed high sensitivity to water quality (e.g., turbidity, phytoplankton blooms), sometimes indicating the presence of water hyacinth when it was absent (e.g., March 2017). SAVI, which is less sensitive to areas under vegetation, did not have this defect and was used to estimate the FVC.

2.2.2. Validation of the Partitioning of Vegetative Cycles

To verify the hypothesis of temporal separation of riparian vegetation cycle and that of water hyacinth, over the years 2017 and 2018, we analyzed the results obtained on two sections of the river located 6.5 km from the estuary and 500 m from each other. These sections were 100 m long and extended across the entire width of the river (Figure 1, red arrow).

Sector 1 is represented the sector without water hyacinth in both years 2017 and 2018, while sector 2 is represented the sector without water hyacinth in 2017 but with water hyacinth in 2018.

A comparison of vegetative area development over two years in both sections could show the difference between the two vegetative cycles.

2.3. Data Processing

2.3.1. Geospatial Data: the Hydrographic Surface Network

We used a Google Earth background image to digitize a hydrographic surface network vector representative of the river corridor from the estuary to the Al Arousse tributary (Table 2). We used an image from March 2013, when the water level was at its highest and the aerial biomass of water hyacinth was not visible. Geographically, the river is long but narrow, which makes it difficult to analyze using remote sensing that has a spatial resolution that is too low.

Table 2. The hydrographic network surface of the studied sections.

Stretch	Length (km)	Width (m)		Area (ha)
		Max.	Min.	
Main Al Kabir River	14.21	80	6	39.5
Al Arousse tributary	2.16	50	1	2.2
Total	16.37			41.7

2.3.2. Remotely-Sensed Data

Sentinel-2 is a pair of multispectral satellites (S2A and S2B, launched in June 2015 and March 2017, respectively) with a revisit time of five days, which provides time series of images (swath: 290 km). These images are accessible online and free of charge [3,54,55]. We only used the red (band 4) and near infrared (band 8) spectral bands with a spatial resolution of 10 m. Sentinel-2 images are downloadable from Operating Platform Sentinel Products (PEPS) [56] and the Continental Surface Data and Services Centre (Theia) [57].

We selected cloud-free images above the entire study area. It is necessary to have reflectance images (BOA—bottom of atmosphere), with a high level of atmospheric correction, the L2A level. When available on download platforms, the L2A level was obtained from the MACCS/MAJA processor. In other cases, we used the Sen2cor processor available on the STEP platform of the European Space Agency (ESA). Image downloading, reflectance value extraction, and data processing were performed with Python.

An amount of 77 Sentinel-2 images have been collected between August 2015 and December 2018 (Table 3). Most of them (34) were collected in 2018 due to the availability of S2B in addition to S2A; in January and February 2018, no images were available due to cloudiness. Pixels in the images were selected if their center laid within the hydrographic surface network (Figure 2).

Table 3. Number of Sentinel-2 images of the study area obtained by month and year.

Year	J	F	M	A	M	J	J	A	S	O	N	D	Total
2015								1	1		1	2	5
2016		1	1	4		2		2	3	3	2		18
2017	1	1	1	1	2	2	1	3	2	1	3	1	19
2018			2	4	6	3	5	5	3	3	2	1	34
Total													77

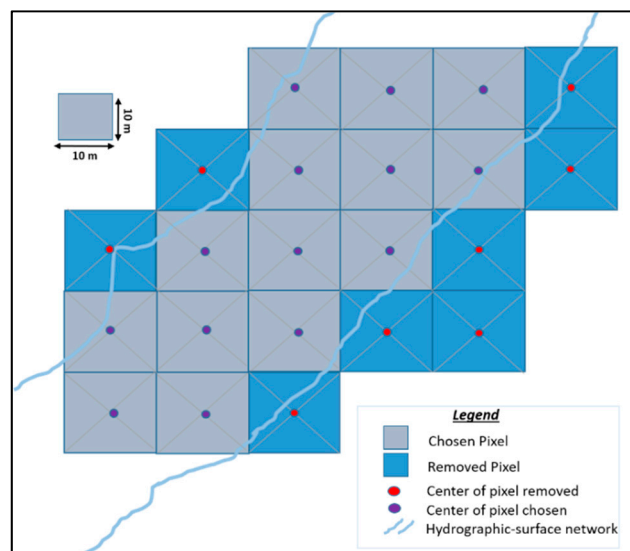


Figure 2. Selection of Sentinel-2 pixels in the surface hydrographic network.

2.3.3. Estimation of the Fractional Vegetation Cover

- Fractional vegetation cover calculation

For the method we developed (Figure 3), we calculated FVC based on SAVI [47], which is calculated as:

$$SAVI_n = \frac{\rho_{NIR} - \rho_R}{\rho_{NIR} + \rho_R + L} (1 + L) \quad (1)$$

where n is the date, ρ_{NIR} is the reflectance value of the near infrared band, ρ_R is the reflectance of the red band, and L is a canopy background adjustment factor (equal to 0.5).

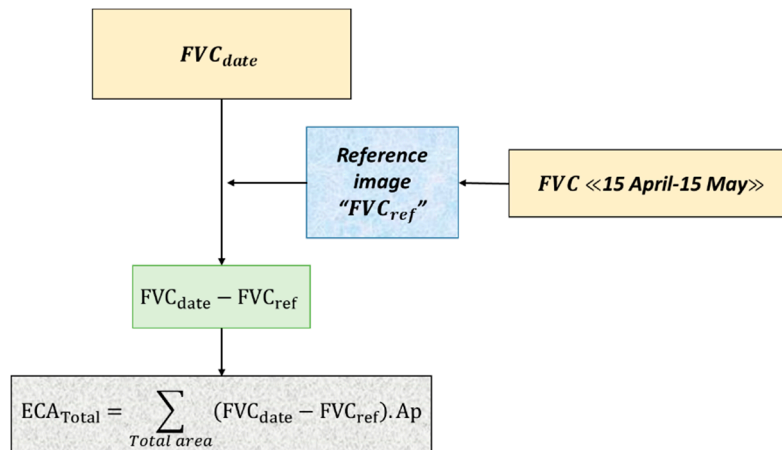


Figure 3. Flowchart for calculating the total area of *Eichhornia crassipes* (ECA_{total}) in the river corridor.

An L value of 0.5 in reflectance space minimized variations in soil and water brightness and eliminated the need for additional calibration for different soils. The transformation was found to nearly eliminate soil-induced variations in vegetation indices. FVC is calculated as:

$$FVC_n = \frac{SAVI_n - SAVI_{min}}{SAVI_{max} - SAVI_{min}} \quad (2)$$

where $SAVI_{min}$ and $SAVI_{max}$ are minimum and maximum values of SAVI, respectively.

To specify $SAVI_{max}$, we made a spectral library of $SAVI_{max}$ values for all available satellite images, which yielded the $SAVI_{max}$ value that corresponded to a pixel completely covered by vegetation.

The $SAVI_{max}$ value observed over an image time series is $SAVI_{max} = 0.9$. This value characterizes a pixel containing only active vegetation that completely covers soil and water. It is not present in all images, particularly those of the winter and early spring periods, when hyacinth is not present and riparian vegetation is not developed. It is, therefore, necessary to search for this value in all available images, mainly in the summer period, and to use that value systematically on each of the dates during the year.

The $SAVI_{min}$ value was set to 0. This minimum value corresponds to the absence of vegetation, i.e., a surface of water or bare soil [47]. Negative values observed on water surfaces correspond to a lack of vegetation, i.e., a value of FVC = 0. Similarly, on bare soils, SAVI values are close to 0, so we have retained the $SAVI_{min}$ value of 0.

- Reference image

The reference period, between mid-April and mid-May, was used as the basis for estimating water hyacinth areas. Knowledge of the baseline condition of the river corridor is therefore required on an annual basis. The availability of Sentinel-2 images is not ensured every year due to cloud conditions, such as in May 2016. It is then necessary to create a synthetic image from the existing images during this period, which will provide a reference that can be used each year.

The calculation of the reference image was only performed with Sentinel-2A images. Indeed, the geographical positioning of Sentinel-2B does not exactly correspond to that of Sentinel-2A, thus creating an artificial dispersion at the pixel scale. Seven Sentinel-2A images were selected: 16 and 26 April 2016; 21 April and 11 May 2017; 16 April, 6 May and 16 May 2018.

From the SAVI_n of each of the seven images ($1 \leq n \leq 7$), a mean SAVI (SAVI_{ref}) was calculated and used to calculate the FVC at the sub-pixel level of the reference image (FVC_{ref}), which was used to calculate the area colonized by water hyacinth:

$$FVC_{ref} = \frac{SAVI_{ref} - SAVI_{min}}{SAVI_{max} - SAVI_{min}} \quad (3)$$

- Area colonized by water hyacinth

Any increase in FVC values after the reference period was due mainly to the appearance and spread of water hyacinth in the river. The area colonized by water hyacinth was detected by calculating the difference between FVC_n on each date and FVC_{ref}. To determine the total area that water hyacinth colonized (ECA_{Total}, m²) over the four years and its annual and inter-annual variation, a simple difference was calculated:

$$ECA_{Total} = \sum_{Total\ Area} (FVC_n - FVC_{ref}) \times A_p \quad (4)$$

where:

ECA_{Total}: Total *Eichhornia crassipes* area on the river

FVC_n: Pixel Fractional Vegetation Cover value at the date n

FVC_{ref}: Pixel Fractional Vegetation Cover of the reference image

A_p: pixel area (100 m²)

- Validation of the water hyacinth surface area estimation model

Validation of the water hyacinth surface area estimation model is difficult to perform in situ due to the current danger at the site located on the border with Syria.

In this context, we have chosen two validation methods:

The first one is to compare the estimated water hyacinth surface area values with manually digitized observations on Google Earth.

The rapid development and movement of water hyacinth's massifs requires Sentinel-2 and Google Earth images to be available at short notice; we have selected 3 October 2016 for Sentinel-2 and 4 October 2016 for Google Earth. The second constraint is to select areas of the river on which water hyacinth differs significantly from other vegetation on the Google Earth image; we have thus retained the part of the river near the estuary.

As previously, the initial river corridor, digitized in winter with high water levels, was divided into 100 m long sections and the first 20 sections were selected from the estuary, i.e., a 2 km analysis. For each section, the areas estimated by Sentinel-2 and Google Earth are calculated.

Two parameters were used to evaluate the accuracy of the model: the root mean square error of prediction (RMSEP), which is the prediction error of the model by comparing the estimated values and those evaluated with Google Earth and the linear correlation coefficient between these same data.

The second one is to estimate FVC from in-situ spot observations. We compared the estimated values of FVC with photographs taken from the Lebanese side. It is a qualitative validation approach based on a comparison of two contrasting years, 2017 with a low water hyacinth development and 2018 with a high water hyacinth development. We selected three sites, photographed in 2017 and 2018 at close dates; Sentinel-2 images are selected at the closest available dates, the difference not exceeding 6 days.

3. Results

3.1. Vegetation of Al Kabir River

Table 4, lists the vegetation observed during field visits with the biological type of each species. Majority of plants developed in the river bed and on banks from the end of January to mid-April and stabilized during the reference period, as for example: *Typha latifolia*, *Salix spp.*, *Xanthium strumarium*. After that water hyacinth developed and colonized the water bodies where it formed a dense carpet and dominated other vegetation that can coexist with it like *Ludwigia stolonifera* or *Lemna minor*.

Table 4. Presence (+) or absence (–) of plant species at the two sites of the study area in 2017–2018.

Scientific Name	Site		Type
	Al Aarida	Hoker ed Dahri	
<i>Alternanthera sessilis</i> (L.) R.Br	+	+	Amphibious (Invasive)
<i>Ludwigia stolonifera</i> Guill. & Perr.	-	+	Amphibious
<i>Lythrum salicaria</i> L.	-	+	Amphibious
<i>Paspalum</i> sp.	+	+	Amphibious
<i>Paspalum distichum</i> L.	-	+	Amphibious (Invasive)
<i>Polygonum salicifolium</i> Wild.	-	+	Amphibious
<i>Typha latifolia</i> L.	+	-	Amphibious
<i>Eichhornia crassipes</i> (Mart.) Solms	+	+	Aquatic (Invasive)
<i>Enteromorpha</i> sp.	+	-	Aquatic algae
<i>Lemna minor</i> L.	-	+	Aquatic
<i>Myriophyllum spicatum</i> L.	+	-	Aquatic
<i>Arundo donax</i> L.	+	+	Terrestrial
<i>Bidens tripartite</i> L.	-	+	Terrestrial
<i>Calystegia sepium</i> (L.) R. Br	-	+	Terrestrial
<i>Chenopodium</i> sp.	+	-	Terrestrial
<i>Chrysanthemum</i> sp.	+	-	Terrestrial
<i>Foeniculum vulgare</i> Mill.	-	+	Terrestrial
<i>Rubus</i> sp.	-	+	Terrestrial
<i>Salix</i> spp.	-	+	Terrestrial
<i>Senecio</i> sp.	-	+	Terrestrial
<i>Sinapis cf nigra</i> (L.) W.D.J. Koch	-	+	Terrestrial
<i>Xanthium strumarium</i> L.	+	+	Terrestrial (Invasive)

3.2. Effectiveness of the Reference image and Validation of Vegetative Cycle Separation

The FVC values of the seven images from mid-April to mid-May are compared with their mean value, which corresponds to the reference image. The results are presented in Figures 4 and 5.

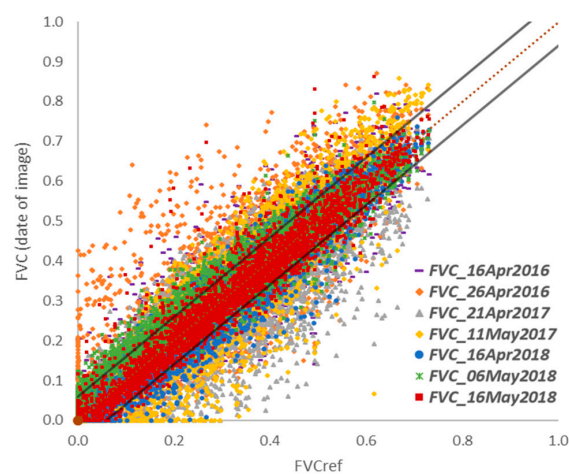


Figure 4. Relationship between the average FVC values of the reference image and those of the component images.

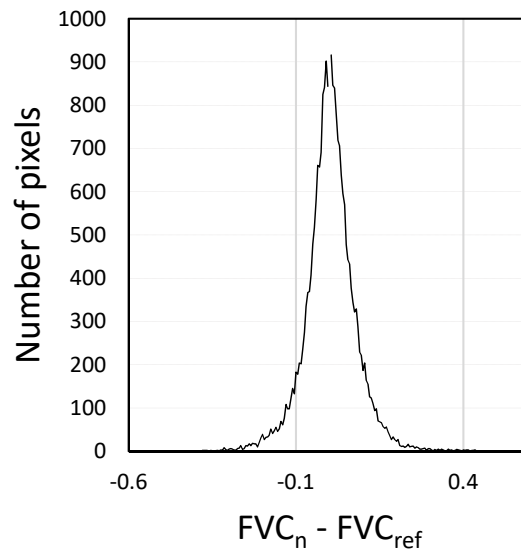


Figure 5. Residue histogram between the FVC values of the component images (FVC_n) and those of their mean (FVC_{ref}).

The dispersion around the mean corresponds to a standard deviation $\sigma = 0.07$. This value represents the interpretable threshold of changes in vegetation cover over time.

The reference image thus makes it possible to calculate the total area of vegetation at that time on the site, i.e., $A_{ref} = 10.5$ ha.

The results of the temporal separation of riparian vegetation cycle and that of water hyacinth are presented in Figure 6.

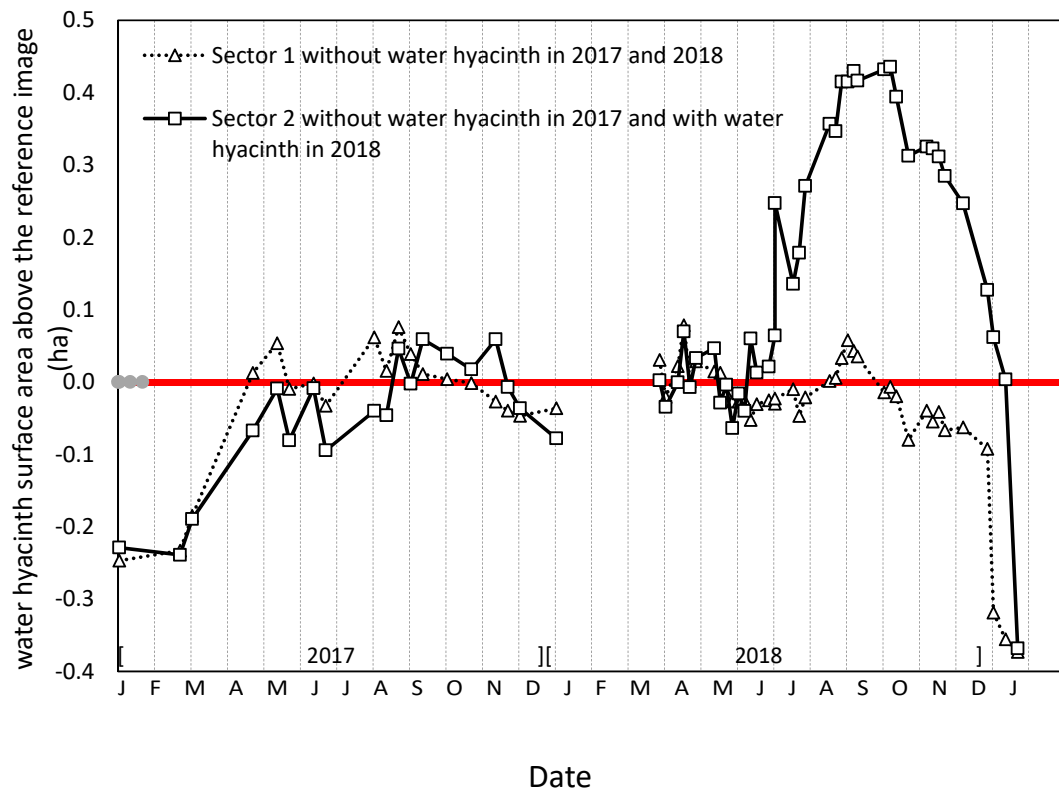


Figure 6. Evolution of the plant surface above the reference value over two 100 m long sectors in the river corridor in 2017 and 2018.

In 2017, neither of these two areas was colonized by water hyacinth and the evolution of the vegetative surface is due only to riparian vegetation. Growth began in February and stabilized from the end of April and finally decreased at the end of November. In 2018, only sector 2 was colonized by water hyacinth while sector 1 remained only with riparian vegetation. The vegetative area in sector 2 increased rapidly from the end of May, at a time when riparian vegetation had stabilized, had peaks in August and September and decreased from October.

The cycle of riparian vegetation and that of water hyacinth therefore appeared to be clearly differentiated over time. Only the fall vegetation decline period was simultaneous, leading to a probable underestimation of the water hyacinth surface area at that time.

3.3. Monthly Dynamics of Fractional Vegetation Cover: 2017 Case Study

Figure 7 shows the monthly situation of the value of the FVC on the river corridor as a function of that of the reference image. As seen above, the growing cycles appear on the images with the well represented reference period in April and May. Prior to this period, the lowest FVC values and variability are in February, reflecting high water levels and little active vegetation in the corridor. After this date, vegetation develops until it reaches a second homogeneous situation in May, at the end of the reference period. From June to January, the variability of FVC in the corridor becomes significant, reflecting major changes in vegetation.

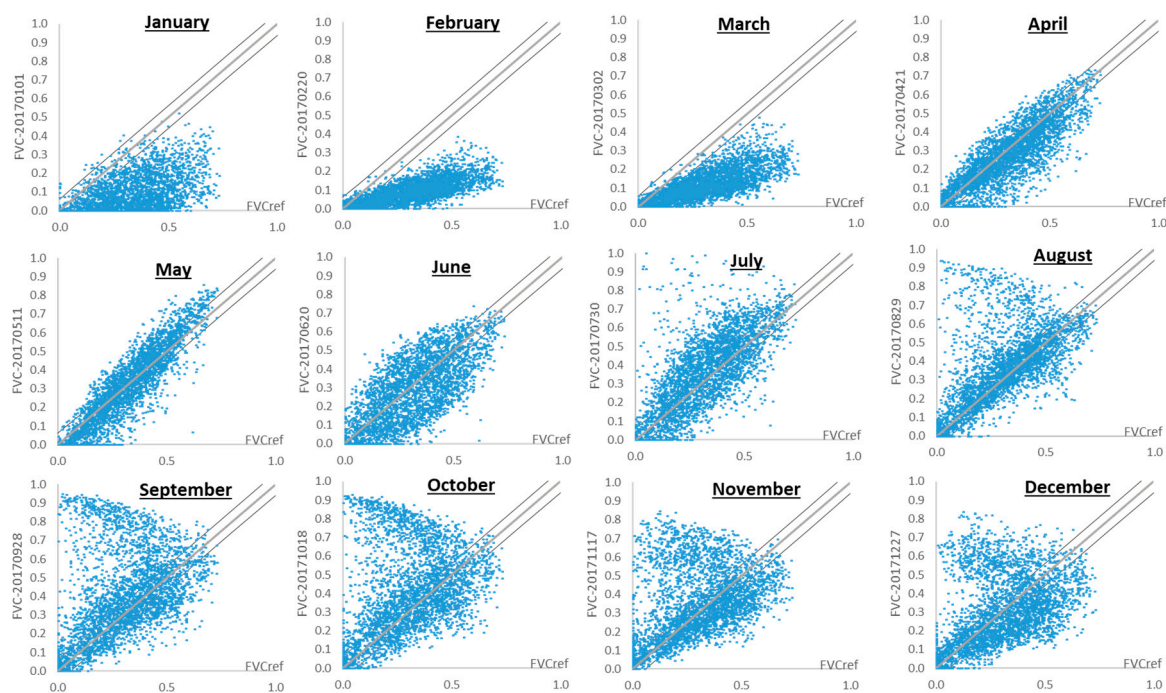


Figure 7. Monthly dynamics of fractional vegetation cover (FVC) in 2017 in relation to the FVC of the reference image (FVCref).

First, in June, the variability of FVC values increases, with some values lower than those of the reference period. One possible explanation is the disappearance of floating and submerged macrophytes that develop in spring and then disappear.

From July to December, a second type of variability appears, in connection with the development of water hyacinth, which intensifies to reach a maximum between September and October. This result reflects, on one hand, that water hyacinth most often colonizes the entire corridor locally and, on the other hand, that this development is all the more important because riparian vegetation is sparsely developed. Then, from November to January, riparian vegetation and water hyacinth decrease simultaneously to reach the lowest level in February.

3.4. Inter-Year Comparison of the Fractional Vegetation Cover (2015–2018)

Figure 8, shows the results obtained over 4 years, from 2015 to 2018, in March, April, August, and November. Spring variability is lower in 2018 than in 2016 and 2017.

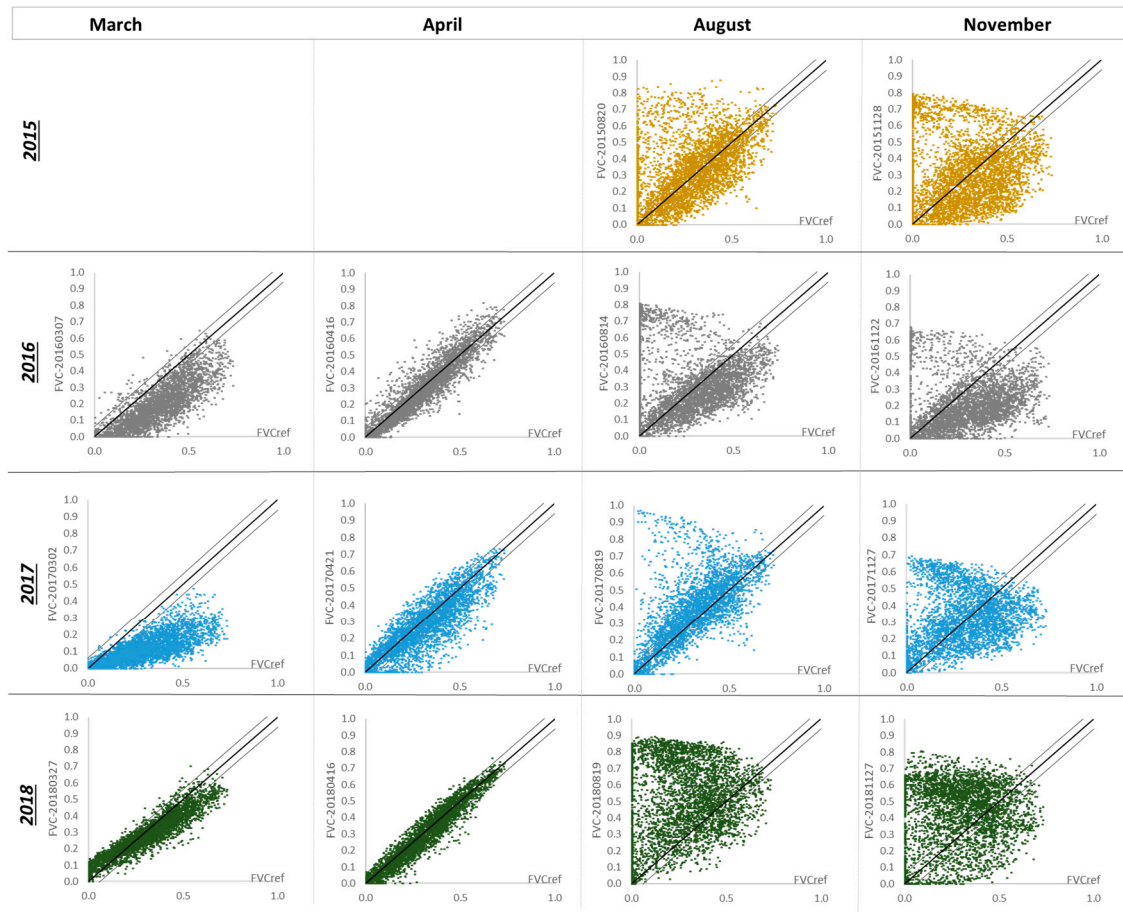


Figure 8. Inter-annual comparison (2015–2018) of fractional vegetation cover (FVC) compared to FVC of the reference image (FVCref) in March, April, August, and November of each year.

In August, water hyacinth developed differently from year to year, with a time delay in water hyacinth's development in 2017 by a lower number of points above riparian vegetation. In 2018, water hyacinth's development was the most important and the reduction in the number of points in the reference image area, i.e., close to the first bisector, indicates that the FVC has been modified over a large part of the river corridor by water hyacinth's development.

In November, all vegetation in the river corridor gradually declined.

3.5. Dynamics of Water Hyacinth Area in the River

Figure 9, shows the evolution of plant surfaces throughout the Al Kabir River corridor over the four years of the study, with a separation between riparian vegetation and water hyacinth.

Before the reference period, riparian vegetation developed similarly in 2016 and 2017, covering ca. 7 ha by mid-March. Riparian vegetation appears to have developed earlier in 2018, since the earliest image available (22 March) indicates a vegetation area of 11.3 ha. A plateau in vegetation area, observed in late spring in 2017 (21 April–10 June) and 2018 (22 March–31 May) seems to confirm the relevance of an intermediate reference period between the development of riparian vegetation and that of water hyacinth.

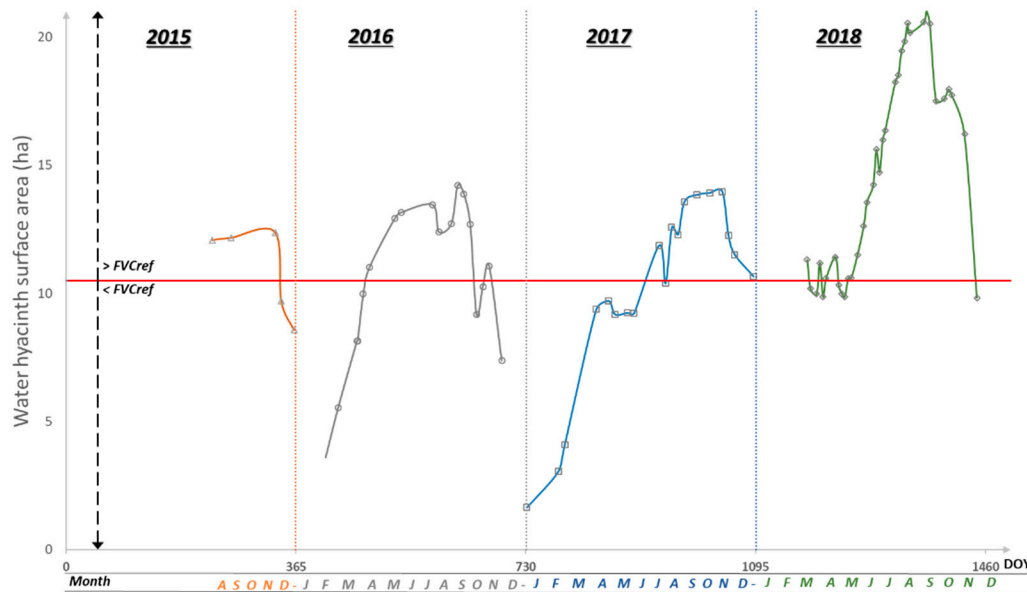


Figure 9. Multi-year dynamics (2015–2018) of the plant surface (ha) in the river corridor. The horizontal red line indicates the FVC threshold of the reference image (FVCref). The areas above this reference value indicate the area of water hyacinth.

The beginning of water hyacinth development also varied among years: Figure 10a, shows significant differences between years. In 2016, water hyacinth developed from 21 April (DOY 111) while in 2017, water hyacinth’s development was later and began on 10 July (DOY 191) and 2018 was an intermediate year (31 May, DOY 151).

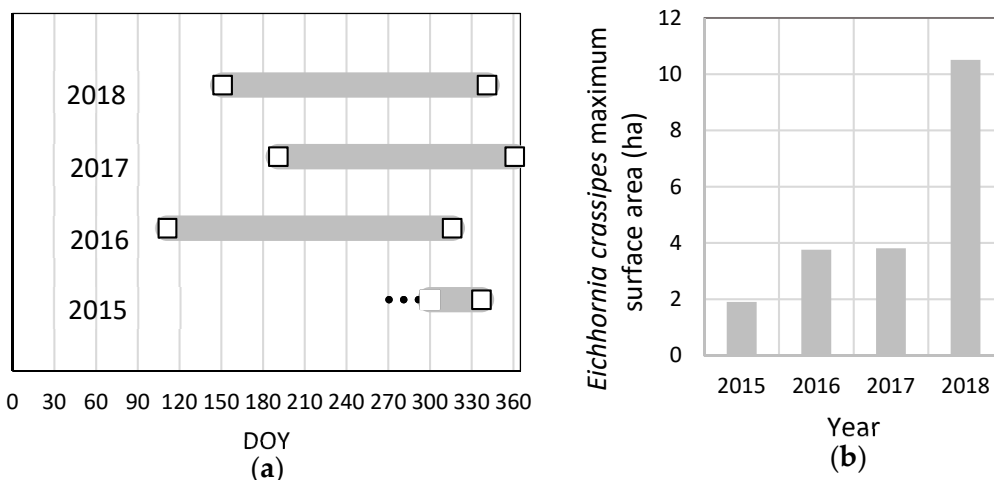


Figure 10. Interannual comparison of the development of *Eichhornia crassipes*. (a) Duration of the period of presence of *Eichhornia crassipes* in the river corridor. (b) Maximum surface area covered during the year (ha).

The most significant difference between years is the total area colonized by water hyacinth. The maximum value of this area reached 10.5 ha in 2018, 3.8 ha in 2016 and 2017, and 1.9 ha in 2015 (Figure 10b).

The autumn decline in vegetation area also varied among years, starting earlier in 2016 than in 2017. Water hyacinth’s end of presence dates followed the same ranking as water hyacinth onset dates, with less significant date differences. The earlier the appearance of water hyacinth, the longer the period during which water hyacinth was present. Thus, more water hyacinth remained at the end of 2017, which greatly increased the area it colonized in 2018.

As well, the spatial distribution of water hyacinth in September 2015–2018 around S1 station assessing locally these differences between years as well as its unequal distribution (Figure 11).

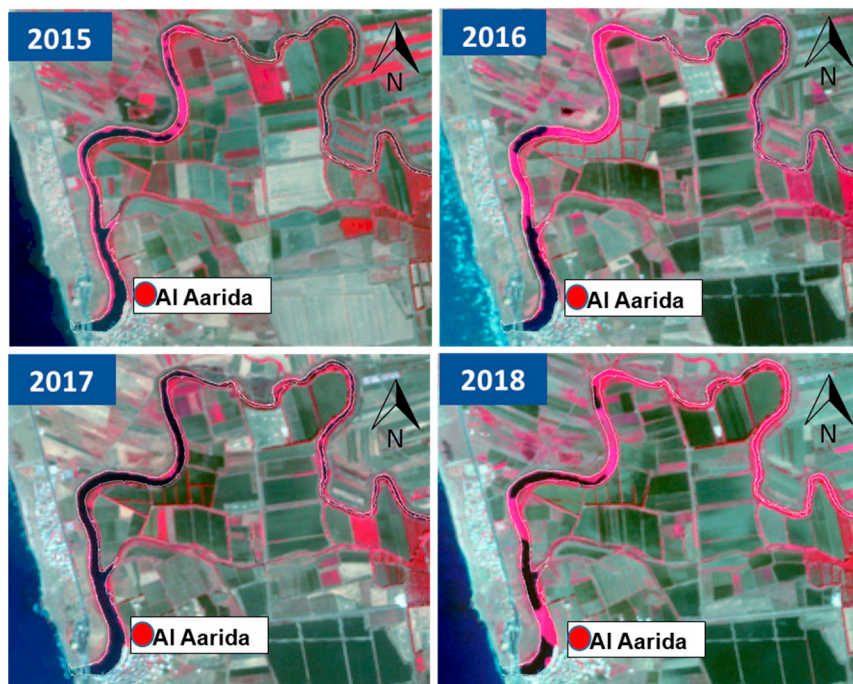


Figure 11. Sentinel-2 images from September of 2015–2018 at the Al Aarida site. Magenta areas on the river represent water hyacinth cover.

3.6. Validation of Water Hyacinth Surface Area Estimation Model

3.6.1. Comparison of the Estimated Water Hyacinth Surface Area Values with Manually Digitized Observations on Google Earth

Figure 12, shows the relationship between the estimated water hyacinth surface values and those observed on Google Earth has a prediction error RMSEP = 0.059 ha and the linear correlation coefficient between these two sets of values is $R = 0.97$. The RMSEP value corresponds to the prediction error of the water hyacinth surface area in hectares over a length of 100 m along the river.

However, differences are still observable between the predicted and observed values: For high water hyacinth surface values, the estimated results are lower than digitalized ones and for low surface values, the model seems to overestimate the digitized values.

To extract water hyacinth surfaces from Google Earth, we have at hand the location of the river banks in winter and we easily determine on Google Earth the boundary between the vegetation surface and the open water surface.

Two sources of errors can explain these differences. First, within the total vegetation surface, it is sometimes difficult to separate riparian vegetation from water hyacinth. Indeed, on Google Earth, the color change between these two types of vegetation is progressive and does not always make it possible to determine precisely the exact limit between the two types of vegetation. The limit chosen sometimes tends to retain an overestimated surface of water hyacinth on Google Earth.

Then, errors in the geographical referencing of Google Earth images can explain some differences. This is the case around the estuary where hyacinth water surfaces seem to exceed the river limit in some places. The real water hyacinth surface is then underestimated with Google Earth.

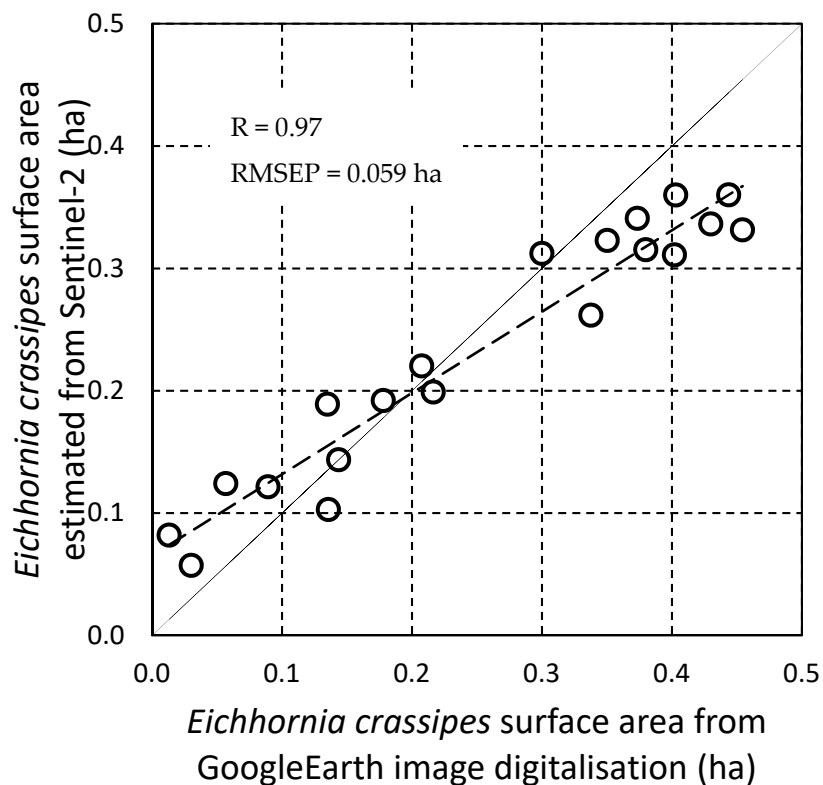


Figure 12. The surface area of *Eichhornia crassipes* obtained by digitizing on Google Earth with that estimated by Sentinel-2.





3.6.2. Estimation of FVC from in Situ Spot Observations

Table 5 shows an overall consistency between the estimated values of FVC and ground observations. Near the estuary, the differences in water hyacinth, development between the two years was marked: water hyacinth surfaces were large in 2018, homogeneous and well distinct from the water surface. Upstream, these FVC differences were reduced, in relation with the narrower width of the river and the greater relative importance of riparian vegetation.

Table 5. Comparison of the development of water hyacinth observed in situ with the values estimated locally by Sentinel-2.

	2017	2018
400 m upstream of the estuary		
Photography Date	25 July 2017	31 July 2018
Sentinel-2 acquisition date	30 July 2017	25 July 2018
Estimated FVC	0	0.8

Table 5. Cont.

	2017	2018
1 km upstream of the estuary		
Photography Date	13 May 2017	4 May 2018
Sentinel-2 acquisition date	11 May 2017	6 May 2018
Estimated FVC	0.05	0.12
9 km upstream of the estuary		
Photography Date	25 July 2017	31 July 2018
Sentinel-2 acquisition date	30 July 2017	25 July 2018
Estimated FVC	0.42	0.53

4. Discussion

The results of our study show the importance of developing a synthetic reference image to detect and quantify the area of water hyacinth colonized during several years. Differences in water hyacinth area among years and the success of this method provide necessary elements to discuss the spread of water hyacinth, with the aim of managing it.

4.1. Fluvial Corridor Geomorphology

The extraction of pixels whose centers were contained in the hydrographic surface network had in some cases over estimated the considered surface area and conversely in other cases, but over the entire network, these differences compensated each other. Information may be inaccessible if the corridor becomes too narrow and does not have pixel centers. However, the use of time series of images compensated for this problem by detecting the dynamics over the entire study area.

The Al Kabir River had a diversity of vegetation cover and changing distribution of water hyacinth. On the Google Earth image used to extract the surface hydrographic network, the water level was high and riparian vegetation was poorly developed. The pixels along the banks had no water hyacinth underneath the riparian vegetation, and these pixels were not kept when we created the hydrographic surface network of the study area. In addition, water hyacinth coexists with other amphibious plants, like *Ludwigia stolonifera*, *Althernanthera sessilis*, and *Paspalum distichum*, and aquatic plants like *Lemna minor*. This association of species was affected by the fast growth of water hyacinth that dominated other species [7]. Such competition could be related to eutrophication which favors the dominance of the water hyacinth.

Then the reflectance detected by satellite images and the evolution of FVC corresponded mainly to the development of water hyacinth.

4.2. Reference Period

Dissociation of vegetative cycles was used as a tool to distinguish water hyacinth from riparian vegetation using Sentinel-2 images. Field observations and comparisons with Google Earth images

confirmed this dissociation and the relevance of choosing Sentinel-2 to build a reference image from multi-year data.

The low standard deviation of the reference image ($\sigma = 0.07$) provides a low detection threshold for a change in vegetation cover and, thus, allows accurate monitoring of water hyacinth development. Only Sentinel-2A images were used to generate the reference image, with Sentinel-2B images providing a dispersion of results. This dispersion is probably related to a slight difference in pixel positioning between the two types of images, but not to radiometric differences between the sensors. However, at the scale of the entire study area, the joint use of Sentinel-2A and Sentinel-2B images outside the reference period should not modify the results but could influence the location of water hyacinth areas along the river. However, this uncertainty would remain in the order of one pixel, which is not important at this resolution (i.e., ca. 10 m).

4.3. Estimation of Fractional Vegetation Cover

The use of FVC in our study seemed to produce consistent results for the detection of vegetation area, as previously demonstrated in the literature [14,58]. In our study, NDVI was sensitive to water turbidity and soil reflectance when the water level was low, as also demonstrated in the literature [14,59]. Consequently, we chose SAVI to calculate the FVC to reduce the effect of soil and water reflectance [49]

4.3.1. Before the Reference Period: Winter and Early Spring

The FVC_n of images compared to the FVC_{ref} demonstrated the dynamics and seasonality of vegetation cover over time.

In winter and early spring, development of water hyacinth could be related to abiotic factors such as increased nutrient availability, temperatures, and light availability [60,61].

In winter, the area of vegetation was low (ca. 1.6 ha in 2017), which corresponded to the loss of leaves of the deciduous riparian vegetation, decrease of herbaceous plants and the rise of the water level in the river. The amount of water hyacinth visible on the surface of the water decreased sharply in winter but did not disappear completely. Low temperatures influence this vegetative decline.

In winter and early spring, another factor explaining differences in water hyacinth area could be the transport and dispersal of plants during floods. Consequently, the water hyacinth area in winter can vary greatly among years (e.g., its largest December area occurred in 2018).

In spring, vegetation cover grew and stabilized by mid-May at the latest, and then water hyacinth appeared and progressively colonized the river to reach its maximum area.

Differences in the growth of water hyacinth and riparian vegetation can occur in some years. If the growth of water hyacinth is early, it can develop at the same time as riparian vegetation. In this case, it will be detected as soon as the total vegetation area exceeds the threshold of the reference image. As long as the reference period is not very far from the assessed period, this detection will be possible even if riparian vegetation is not stabilized.

4.3.2. After the Reference Period: Late Spring to Autumn

In summer and autumn, the abiotic factors favoring the development of water hyacinth are also related to the nutrient and the light availability and to temperature [60,61].

The decrease in FVC in autumn corresponded to two biological processes: senescence and gradual disappearance of water hyacinth and senescence of riparian vegetation.

4.4. Inter-Annual Comparison

The main stages of water hyacinth dynamics remained similar among years, but with differences in the area colonized and development date. Inter-annual differences could be likely due to differences in weather and discharge. In winter, rain influences river flow while, in spring and summer, air temperature influences vegetation growth and development. We observed similar dynamics in total vegetation area among years but with some variability, probably due to flooding and the rate of water

hyacinth development. Another interannual disparity may occur if the water hyacinth surface replaces riparian vegetation. In this case, the method based on an inter-vegetation cycle reference image would result in an underestimation of the water hyacinth surface. The probability of such a change remains low because riparian vegetation is more stable over time than water hyacinth. However, these results first validated the choice of a reference period to compare the development of interannual vegetation, which made it possible to detect and quantify the intra- and interannual area colonized by water hyacinth.

4.5. Further Developments

To supplement this research in future studies, it would be useful to include hydrological and climatic parameters in order to analyze the ecological conditions that influence the spread of water hyacinth. Studying temporal and spatial dynamics of vegetation should help stakeholders develop strategies to manage such ecological invasions. To render estimates of spatial distribution more precise, complementary methods could be used to identify the floristic composition within pixels along riverbanks. In addition, spectral signatures could be obtained for plants that are less developed when field observations occur, followed by hyperspectral images.

4.6. Use for Management

Resource managers can use remote sensing to monitor and quantify areas colonized by invasive plants [62–64], showing the importance of identifying when proliferation begins and where and how much biomass should be removed. Remote sensing and mapping can help to identify appropriate management strategies and assess their effectiveness. To manage the spread and extent of invasive plants, mechanical, physical, and biological methods have been used [12]. Above all, rapid monitoring and management is recognized as one of the most cost-effective ways to determine the locations and invasion strategies against invasive plants [1,41,65–67].

Mechanical methods are those applied most widely to manage water hyacinth over large areas [65]. Mechanical methods to eradicate or limit the spread of water hyacinth and other free-floating plants have had wide success in many European countries and the USA [12]. Mechanical excavation is more useful in narrow water bodies, such as channels, irrigation systems, and small rivers. The ability of this method to eradicate *Ludwigia grandiflora* (Michaux.) Greuter and Burdet in France was tested [12]. A necessary complement to mechanical methods is manual removal, which provides the best results, especially in early stages of invasion. Manual removal has successfully eradicated *L. grandiflora* and *Myriophyllum aquaticum* (Vell.) Verdc. from certain areas [12]. Nonetheless, it requires intensive labor, equipment, and funding; consequently, it is better suited to small areas with small amounts of invasive plants [12].

5. Conclusions

We assessed the potential of Sentinel-2 images to quantify vegetation area. Given their relatively low spatial resolution, we developed a new method to extract information from a time series of images. Water hyacinth cover and dynamics were mapped successfully involving this method. We were also able to distinguish water hyacinth from other vegetation in the river due to differences in their vegetative cycles and development periods. Thus, FVC calculated from SAVI was a pertinent variable to detect changes in vegetation area.

The remote sensing method developed here does not require detailed field observations and can therefore be applied to other regions as long as water hyacinth's development cycle can be distinguished from those of other plants. Sentinel-2 satellites S2A and S2B can be used successfully to monitor water hyacinth development in the climate of the Middle East. The complementarity of the two Sentinel-2 satellites provides a satisfactory time series for annual monitoring of water hyacinth.

Author Contributions: Conceptualization: H.N., J.H., H.A.H., and G.F.; methodology: H.N.; software: P.P.; validation: H.N., Y.G., J.H., H.A.H., and A.F.; formal analysis: Y.G.; investigation: H.N., G.F., H.A.H., J.H., Y.G., A.F.; resources: G.F., A.F.; data curation: P.P.; writing—original draft preparation: Y.G.; writing—review and editing: H.N., J.H., H.A.H., G.F., A.F., and Y.G.; supervision: H.N., G.F., J.H., and H.A.H.; project administration: H.N., J.H., H.A.H., and G.F.

Funding: This research was funded by the Lebanese University and National Research Center (CNRS-L), Lebanon.

Acknowledgments: Particular acknowledgements is due (concern) to Lebanese University, CNRS-L (Lebanon) and Agrocampus-Ouest (France) that supported a collaboration to realize this study.

Conflicts of Interest: The authors declare no conflict of interest.

References

1. Alvarez-Taboada, F.; Paredes, C.; Julián-Pelaz, J. Mapping of the invasive species *Hakea sericea* using Unmanned Aerial Vehicle (UAV) and worldview-2 imagery and an object-oriented approach. *Remote Sens.* **2017**, *9*, 913. [[CrossRef](#)]
2. Gopal, B. *Ecology and Management of Aquatic Vegetation in the Indian Subcontinent*; Springer Science & Business Media: Berlin, Germany, 1987.
3. Thamaga, K.H.; Dube, T. Remote sensing of invasive water hyacinth (*Eichhornia crassipes*): A review on applications and challenges. *Remote Sens. Appl. Soc. Environ.* **2018**, *10*, 36–46. [[CrossRef](#)]
4. Lowe, S.; Browne, M.; Boudjelas, S.; De Poorter, M. *100 of the World's Worst Invasive Alien Species. From A Selection Global. The Database, Invasive Species*; ISCG: Rome, Italy, 2004.
5. Kriticos, D.J.; Brunel, S. Assessing and Managing the Current and Future Pest Risk from Water Hyacinth, (*Eichhornia crassipes*), an Invasive Aquatic Plant Threatening the Environment and Water Security. *PLoS ONE* **2016**, *11*, e0120054. [[CrossRef](#)] [[PubMed](#)]
6. Wilson, J.R.; Holst, N.; Rees, M. Determinants and patterns of population growth in water hyacinth. *Aquat. Bot.* **2005**, *81*, 51–67. [[CrossRef](#)]
7. Téllez, T.; López, E.; Granado, G.; Pérez, E.; López, R.; Guzmán, J. The Water Hyacinth, *Eichhornia crassipes*: An invasive plant in the Guadiana River Basin (Spain). *Aquat. Invasions* **2008**, *3*, 42–53. [[CrossRef](#)]
8. Timmer, C.E.; Weldon, L.W. Evapotranspiration and pollution of water by water hyacinth. *Hyacinth Control J.* **1966**, *6*, 34–37.
9. Mozaffarian, V.; Yaghoubi, B. New record of *Eichhornia crassipes* (Water Hyacinth) from north of Iran. *Rostaniha Agric. Res. Educ. Ext. Organ. Res. Assist. Prof.* **2015**, *16*, 208–211.
10. Dagno, K.; Lahlali, R.; Friel, D.; Bajji, M.; Haïssam Jijakli, M. Synthèse bibliographique: Problématique de la jacinthe d'eau, *Eichhornia crassipes*, dans les régions tropicales et subtropicales du monde, notamment son éradication par la lutte biologique au moyen des phytopathogènes. *Biotechnol. Agron. Soc. Environ.* **2007**, *11*, 144–150.
11. Everitt, J.H.; Yang, C.; Escobar, D.E.; Webster, C.F.; Lonard, R.I.; Davis, M.R. Using remote sensing and spatial information technologies to detect and map two aquatic macrophytes. *J. Aquat. Plant Manag.* **1999**, *37*, 71–80.
12. Hussner, A.; Stiers, I.; Verhofstad, M.J.J.M.; Bakker, E.S.; Grutters, B.M.C.; Haury, J.; Van Valkenburg, J.L.C.H.; Brundu, G.; Newman, J.; Clayton, J.S.; et al. Management and control methods of invasive alien freshwater aquatic plants: A review. *Aquat. Bot.* **2017**, *136*, 112–137. [[CrossRef](#)]
13. Hestir, E.L.; Khanna, S.; Andrew, M.E.; Santos, M.J.; Viers, J.H.; Greenberg, J.A.; Rajapakse, S.S.; Ustin, S.L. Identification of invasive vegetation using hyperspectral remote sensing in the California Delta ecosystem. *Remote Sens. Environ.* **2008**, *112*, 4034–4047. [[CrossRef](#)]
14. Barati, S.; Rayegani, B.; Saati, M.; Sharifi, A.; Nasri, M. Comparison the accuracies of different spectral indices for estimation of vegetation cover fraction in sparse vegetated areas. *Egypt. J. Remote Sens. Space Sci.* **2011**, *14*, 49–56. [[CrossRef](#)]
15. Albright, T.P.; Moorhouse, T.G.; Mcnabb, T.J. The Rise and Fall of Water Hyacinth in Lake Victoria and the Kagera River Basin, 1989–2001. *J. Aquat. Plant Manag.* **2004**, *42*, 73–84.
16. Mund, J.; Murach, D.; Parplies, A. Monitoring and Quantification of Floating Biomass on Tropical Water Bodies. *Geospatial Innov. Soc.* **2014**, 67–76. [[CrossRef](#)]
17. Ogamba, E.N.; Izah, S.C.; Oribu, T. Water quality and proximate analysis of *Eichhornia crassipes* from River Nun, Amassoma Axis, Nigeria. *Res. J. Phytomed.* **2015**, *1*, 43–48.

18. Rommens, W.; Maes, J.; Dekeza, N.; Inghelbrecht, P.; Nhiwatiwa, T.; Holsters, E.; Ollevier, F.; Marshall, B.; Brendonck, L. The impact of water hyacinth (*Eichhornia crassipes*) in a eutrophic subtropical impoundment (Lake Chivero, Zimbabwe). I. Water quality. *Archiv für Hydrobiologie* **2003**, *158*, 373–388. [[CrossRef](#)]
19. Pan, X.; Villamagna, A.M.; Li, B.; Villamagna, A.M.; Li, B. *Eichhornia crassipes* Mart. (Solms-Laubach) (Water Hyacinth). In *A Handbook of Global Freshwater Invasive Species*; Routledge: London, UK, 2012.
20. Patel, S. Threats, management and envisaged utilizations of aquatic weed *Eichhornia crassipes*: An overview. *Rev. Environ. Sci. Biotechnol.* **2012**, *11*, 249–259. [[CrossRef](#)]
21. Venugopal, G. Monitoring the effects of biological control of water hyacinths using remotely sensed data: A case study of Bangalore, India. *Singap. J. Trop. Geogr.* **1998**, *19*, 92–105. [[CrossRef](#)]
22. Uremis, I.; Uludag, A.; Arslan, Z.F.; Abaci, O. A new record for the flora of Turkey: *Eichhornia crassipes* (Mart.) Solms (Pontederiaceae). *EPPO Bull.* **2014**, *44*, 83–86. [[CrossRef](#)]
23. EPPO. EPPO A1 and A2 Lists of Pests Recommended for Regulation as Quarantine Pests. *EPPO Bull.* **2008**, *5*, 205–207.
24. UN-ESCWA; BGR. Naher El Kabir basin. In *Inventory of Shared Water Resources in Western Asia*; United Nations Economic and Social Commission for Western Asia (UN-ESCWA) and the German Federal Institute for Geosciences and Natural Resources (BGR): New York, NY, USA, 2013.
25. García-Berthou, E.; Alcaraz, C.; Pou-Rovira, Q.; Zamora, L.; Coenders, G.; Feo, C. Introduction pathways and establishment rates of invasive aquatic species in Europe. *Can. J. Fish. Aquat. Sci.* **2005**, *62*, 453–463. [[CrossRef](#)]
26. Hussner, A. Alien aquatic plant species in European countries. *Weed Res.* **2012**, *52*, 297–306. [[CrossRef](#)]
27. Mazza, G.; Aquiloni, L.; Inghilesi, A.F.; Giuliani, C.; Lazzaro, L.; Ferretti, G.; Lastrucci, L.; Foggi, B.; Tricarico, E. Aliens just a click away: The online aquarium trade in Italy. *Manag. Biol. Invasions* **2015**, *6*, 253–261. [[CrossRef](#)]
28. Celesti-Grapow, L.; Alessandrini, A.; Arrigoni, P.V.; Banfi, E.; Bernardo, L.; Bovio, M.; Brundu, G.; Cagiotti, M.R.; Camarda, I.; Carli, E.; et al. Inventory of the non native flora of Italy. *Plant Biosyst.* **2009**, *143*, 386–430. [[CrossRef](#)]
29. Brundu, G.; Azzella, M.M.; Blasi, C.; Camarda, I.; Iberite, M.; Celesti-Grapow, L. The silent invasion of *Eichhornia crassipes* (Mart.) Solms. in Italy. *Plant Biosyst.* **2013**, *147*, 1120–1127. [[CrossRef](#)]
30. Georges, N.; Pax, N. *Pistia stratiotes* L. et *Eichhornia crassipes* (Mart) Solms, deux nouvelles hydrophytes dans la vallée de la Moselle. *Bull. Liaison Floraine* **2002**, *28*, 3–4.
31. Perna, C.; Burrows, D. Improved dissolved oxygen status following removal of exotic weed mats in important fish habitat lagoons of the tropical Burdekin River floodplain, Australia. *Mar. Pollut. Bull.* **2005**, *51*, 138–148. [[CrossRef](#)] [[PubMed](#)]
32. IDRC. *Cad Ham*; Cadham Hayes Systems Inc: Ottawa, ON, Canada, 2003; p. 108.
33. Thomas, R.L.; Shaban, A.; Khawlie, M.; Kawass, I.; Nsouli, B. Geochemistry of the sediments of the El-Kabir River and Akkar watershed in Syria and Lebanon. *Lakes Reserv. Res. Manag.* **2005**, *10*, 127–134. [[CrossRef](#)]
34. Guyet, T.; Nicolas, H. Long term analysis of time series of satellite images. *Pattern Recognit. Lett.* **2015**, *70*, 17–23. [[CrossRef](#)]
35. Schmidt, M. Monitoring aquatic weeds in a river system using SPOT 5 satellite imagery. *J. Appl. Remote Sens.* **2010**, *4*, 043528. [[CrossRef](#)]
36. Santos, M.J.; Khanna, S.; Hestir, E.L.; Andrew, M.E.; Rajapakse, S.S.; Greenberg, J.A.; Anderson, L.W.; Ustin, S.L. Use of Hyperspectral Remote Sensing to Evaluate Efficacy of Aquatic Plant Management. *Invasive Plant Sci. Manag.* **2009**, *2*, 216–229. [[CrossRef](#)]
37. Jakubauskas, M.E.; Peterson, D.L.; Campbell, S.W.; de Noyelles, F.; Campbell, S.D.; Penny, D. Mapping and monitoring invasive aquatic plant obstructions in navigable waterways using satellite multispectral imagery. In Proceedings of the Pecora 15 Land Satellite Information IV Conference and the ISPRS Commission I Symposium, Denver, CO, USA, 10–15 November 2002.
38. Everitt, J.H.; Yang, C.H. Using QuickBird satellite imagery to distinguish two aquatic weeds in south Texas. *J. Aquat. Plant Manag.* **2007**, *45*, 25–31.
39. Oyama, Y.; Matsushita, B.; Fukushima, T. Distinguishing surface cyanobacterial blooms and aquatic macrophytes using Landsat/TM and ETM+ shortwave infrared bands. *Remote Sens. Environ.* **2015**, *157*, 35–47. [[CrossRef](#)]

40. Fadel, A.; Faour, G.; Slim, K. Assessment of the trophic state and chlorophyll-a concentrations using landsat oli in karaoun reservoir, Lebanon. *Leban. Sci. J.* **2016**, *17*, 130–145. [[CrossRef](#)]
41. Dube, T.; Mutanga, O.; Sibanda, M.; Bangamwabo, V.; Shoko, C. Evaluating the performance of the newly-launched Landsat 8 sensor in detecting and mapping the spatial configuration of water hyacinth (*Eichhornia crassipes*) in inland lakes, Zimbabwe. *Phys. Chem. Earth* **2017**, *100*, 101–111. [[CrossRef](#)]
42. Pinardi, M.; Bresciani, M.; Villa, P.; Cazzaniga, I.; Laini, A.; Tóth, V.; Fadel, A.; Austoni, M.; Lami, A.; Giardino, C. Spatial and temporal dynamics of primary producers in shallow lakes as seen from space: Intra-annual observations from Sentinel-2A. *Limnologica* **2018**, *72*, 32–43. [[CrossRef](#)]
43. Colombo, R.; Bellingeri, D.; Fasolini, D.; Marino, C.M. Retrieval of leaf area index in different vegetation types using high resolution satellite data. *Remote Sens. Environ.* **2003**, *86*, 120–131. [[CrossRef](#)]
44. Rouse, J.W.; Haas, R.H.; Schell, J.A.; Deering, D.W.; Harlan, J.C. *Monitoring the Vernal Advancements and Retrogradation of Natural Vegetation*; Remote Sensing Center: College Station, TX, USA, 1974.
45. Broge, N.H.; Leblanc, E. Comparing prediction power and stability of broadband and hyperspectral vegetation indices for estimation of green leaf area index and canopy chlorophyll density. *Remote Sens. Environ.* **2000**, *76*, 156–172. [[CrossRef](#)]
46. Jackson, R.D.; Huete, A.R. Interpreting vegetation indices. *Prev. Vet. Med.* **1991**, *11*, 185–200. [[CrossRef](#)]
47. Bronge, L.B.; SwedPower, A.B. *Satellite Remote Sensing for Estimating Leaf Area Index, FPAR and Primary Production*; Swedish Nuclear Fuel and Waste Management: Stockholm, Sweden, 2004.
48. Huete, A.R. A soil-adjusted vegetation index (SAVI). *Remote Sens. Environ.* **1988**, *25*, 295–309. [[CrossRef](#)]
49. Almutairi, B.; El, A.; Belaid, M.A.; Musa, N. Comparative Study of SAVI and NDVI Vegetation Indices in Sulaibiya Area (Kuwait) Using Worldview Satellite Imagery. *Int. J. Geosci. Geomatics* **2013**, *1*, 50–53.
50. Zhang, X.; Liao, C.; Li, J.; Sun, Q. Fractional vegetation cover estimation in arid and semi-arid environments using HJ-1 satellite hyperspectral data. *Int. J. Appl. Earth Obs. Geoinf.* **2012**, *21*, 7. [[CrossRef](#)]
51. Jiménez-Muñoz, J.C.; Sobrino, J.A.; Plaza, A.; Guanter, L.; Moreno, J.; Martínez, P. Comparison between fractional vegetation cover retrievals from vegetation indices and spectral mixture analysis: Case study of PROBA/CHRIS data over an agricultural area. *Sensors* **2009**, *9*, 768–793. [[CrossRef](#)] [[PubMed](#)]
52. Wu, D.; Wu, H.; Zhao, X.; Zhou, T.; Tang, B.; Zhao, W.; Jia, K. Evaluation of Spatiotemporal Variations of Global Fractional Vegetation Cover Based on GIMMS NDVI Data from 1982 to 2011. *Remote Sens.* **2014**, *6*, 4217–4239. [[CrossRef](#)]
53. Jia, K.; Liang, S.; Liu, S.; Li, Y.; Xiao, Z.; Yao, Y.; Jiang, B.; Zhao, X.; Wang, X.; Xu, S.; et al. Global Land Surface Fractional Vegetation Cover Estimation Using General Regression Neural Networks From MODIS Surface Reflectance. *IEEE Trans. Geosci. Remote Sens.* **2015**, *53*, 4787–4796. [[CrossRef](#)]
54. ESA. *Sentinel-2 ESA's Optical High-Resolution Mission for GMES Operational Services*. PO Box 299, 2200 AG; ESA Communications ESTEC: Noordwijk, The Netherlands, 2012.
55. Tello, J.; Gómez-Báguena, R.; Casterad, M.A. Comparison and adjustment in agricultural areas of vegetation indexes derived from Landsat-8 and Sentinel-2. In Proceedings of the Nuevas Plataformas y Sensores Teledetección—XVII Congreso de la Asociación Española de Teledetección, Murcia, Spain, 3–7 October 2017; pp. 81–84.
56. PEPS. PEPS—Operating platform Sentinel products (CNES). Available online: <https://peps.cnes.fr> (accessed on 28 June 2019).
57. Theia. Theia—The Continental Surface Data and Services Center. Available online: <https://theia.cnes.fr> (accessed on 28 June 2019).
58. Vescovo, L.; Gianelle, D. Using the MIR bands in vegetation indices for the estimation of grassland biophysical parameters from satellite remote sensing in the Alps region of Trentino (Italy). *Adv. Space Res.* **2008**, *41*, 1764–1772. [[CrossRef](#)]
59. Eid, E.M.; Shaltout, K.H. Population dynamics of *Eichhornia crassipes* (C. Mart.) Solms in the Nile Delta, Egypt. *Plant Spec. Biol.* **2016**, *32*, 279–291. [[CrossRef](#)]
60. Batanouny, K.H.; El-Fiky, A.M. The water hyacinth (*Eichhornia crassipes* Solms) in the Nile system, Egypt. *Aquat. Bot.* **1975**, *1*, 243–252. [[CrossRef](#)]
61. Yan, S.-H.; Song, W.; Guo, J.-Y. Advances in management and utilization of invasive water hyacinth (*Eichhornia crassipes*) in aquatic ecosystems—A review. *Crit. Rev. Biotechnol.* **2017**, *37*, 218–228. [[CrossRef](#)]
62. Bottner, B.; Noël, C. Repérer les macrophytes depuis le ciel ou sous les eaux, quel appui pour les gestionnaires? *Sci. Eaux Territ.* **2014**, *15*, 10–15.

63. Varray, S.; Haury, J.; Hudin, S. *Manuel de Gestion des Espèces Exotiques Envahissantes du Bassin Loire-Bretagne*; Fédération des Conservatoires d’Espaces Naturels: Orléans, France, 2018.
64. Dutartre, A.; Haury, J.; Peltre, M.-C. *Plantes Aquatiques d’eau Douce: Biologie, Écologie et Gestion*. Cemagref HS Rev. *Ingénierie Eau-Agriculture-Territoire*; Irstea: Villeurbanne, France, 2008; p. 161.
65. Joshi, C.; de Leeuw, J.; van Duren, I.C. Remote Sensing and GIS Applications for Mapping and Spatial Modelling of Invasive Species. *Geoinf. Sci.* **2002**, *2*, 669–677.
66. Laranjeira, C.M.; Nadais, G. *Eichhornia crassipes* control in the largest Portuguese natural freshwater lagoon. *EPPO Bull.* **2008**, *38*, 487–495. [[CrossRef](#)]
67. Haury, J.; Damien, J.-P. De nouvelles mauvaises herbes en zones humides: Les formes terrestres des Jussies invasives sur prairies. *Sciences Eaux Territoires* **2014**, *15*, 16–21.



© 2019 by the authors. Licensee MDPI, Basel, Switzerland. This article is an open access article distributed under the terms and conditions of the Creative Commons Attribution (CC BY) license (<http://creativecommons.org/licenses/by/4.0/>).